Ecological Modelling 479 (2023) 110310

Contents lists available at ScienceDirect

Ecological Modelling

journal homepage: www.elsevier.com/locate/ecolmodel

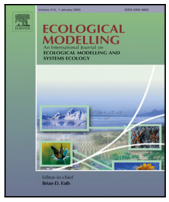

Fluctuation of growth and photosynthetic characteristics in *Prorocentrum shikokuense* under phosphorus limitation: Evidence from field and laboratory

Anglu Shen [a,1], Shufei Gao [b,1], Christopher M. Heggerud [c], Hao Wang [d], Zengling Ma [e], Sanling Yuan [b,*]

[a] College of Marine Ecology and Environment, Shanghai Ocean University, Shanghai 201306, China
[b] College of science, University of Shanghai for Science and Technology, Shanghai 200093, China
[c] Department of Environmental Science and Policy, University of California, Davis, CA 95616, United States
[d] Department of Mathematical and Statistical Sciences, University of Alberta, Edmonton, Alberta T6G 2G1, Canada
[e] Zhejiang Provincial Key Laboratory for Subtropical Water Environment and Marine Biological Resources Protection, Wenzhou University, Wenzhou 325035, China

ARTICLE INFO

Keywords:
Algal bloom
Prorocentrum shikokuense
Chlorophyll fluorescence
Fluctuation
Model fitting

ABSTRACT

Exploring the complex interaction between algal growth and their photo-physiology is of significant interest as it can further the understanding of harmful algal blooms. To this end, we investigate variations in cell abundance and chlorophyll fluorescence parameters during the algal bloom formation of *Prorocentrum shikokuense* in the field and batch culture via the pulse amplitude modulated fluorometry. Furthermore, based on the interaction between algal growth and its photo-physiology status, we develop a novel algal growth model incorporating cell growth delay. The model parameters are estimated by fitting the experimental data of *P. shikokuense* and validated by the experimental data of *Symbiodinium* sp. The experimental results show that the growth status and photosynthetic parameters of algal cells fluctuate in both field and laboratory experiments and that the photosynthetic parameters have a faster response than growth parameters. According to the experimental and mathematical results, the time delay between the slow growth of algae and the rapid change of photosynthetic parameters may be a physiological mechanism leading to the fluctuations in algal growth. These results are significant for studying the relationship between phytoplankton growth dynamics and photosynthetic parameters and will help resource managers to predict and deepen the understanding of harmful algal blooms.

1. Introduction

In the East China Sea (ECS), the species of dinoflagellates *Prorocentrum shikokuense* (formerly named *P. donghaiense*; (Shin et al., 2019; Gómez et al., 2021; Lu et al., 2022)) frequently forms harmful algal blooms (HABs) in the late spring and early summer that last for weeks or months. These HABs have occurred annually since 2000 and have adverse effects on the coastal area from the estuary of Changjiang River down to Fujian Province, China (Lu et al., 2022; Chen and Chen, 2021). The frequency and severity of *P. shikokuense* HABs have resulted in significant ecological damages, such as plankton community structure changes (Chai et al., 2020; Chen et al., 2020; Lin et al., 2014; Shen et al., 2019, 2022). Furthermore, these detrimental impacts of *P. shikokuense* blooms include a decreased abundance of copepods (good food organisms for fish) accompanied by an increased abundance of small jellyfish, which will inevitably affect the fishery resources leading to economic losses (Lin et al., 2014; Shen et al., 2022). An outbreak of dinoflagellates blooms (e.g. *P. shikokuense*) has been observed on the coast of ECS after the spring diatom blooms and is often accompanied by low orthophosphate (P_i) levels (Kong et al., 2016; Wang et al., 2019; Zhang et al., 2019b,a). This is because dinoflagellates have strategies for assimilating and storing different resources as pools (nitrogen, phosphorus, and trace elements) (Kustka et al., 2003; Jiang et al., 2019; Qi et al., 2013). While both diatoms and dinoflagellates can store polymers of P_i, the larger size of dinoflagellates may have a greater cell P_i storage capacity, allowing some dinoflagellates to maintain a relatively high growth rate under a low P_i environment (Hou et al., 2007; Diaz et al., 2008). In addition, *P. shikokuense* using organic forms of phosphorus is an important adaptive strategy under phosphorus limitation (Ou et al., 2008; Zhang et al., 2019c). Significant evidence suggests that dissolved organic phosphorus is an important source of

* Corresponding author.
E-mail address: sanling@usst.edu.cn (S. Yuan).
[1] Co-first author

https://doi.org/10.1016/j.ecolmodel.2023.110310
Received 29 September 2022; Received in revised form 9 January 2023; Accepted 5 February 2023

phytoplankton phosphorus in low P_i areas (Mclaughlin et al., 2013; Wu et al., 2000). Remote sensing or field investigations have shown a very high abundance of *P. shikokuense* in every bloom formation, between May and June, in the ECS since the year 2000 (Lin et al., 2014; Shen et al., 2019; Tao et al., 2015, 2017; Lu et al., 2022). Therefore, *P. shikokuense* has been a key research species in the field of HABs in the ECS during the last two decades (Lu et al., 2022).

Photosynthesis (affected by phosphorus) is the dominant factor in algal growth and reproduction. Chlorophyll *a* (Chl*a*) concentration, maximal quantum yield (F_v/F_m), actual quantum yield (F'_q/F'_m), efficiency of electron transport (α), and maximum relative electron transport rate ($rETR_{max}$) are important evaluation indexes of photosynthesis as they describe many photosynthetic characteristics. F_v/F_m indicate that the intrinsic light energy conversion efficiency of PSII reaction center is measured after leaf dark adaptation for 20 min. Under non-stress conditions, the change of this parameter is very little and is not affected by species and growth conditions, while under stress conditions, the parameter decreases significantly (Xu et al., 1992). F'_q/F'_m reflects the actual light energy capture efficiency of the PSII reaction center in the case of partial closure, which is measured directly without dark adaptation. Several studies indicate that F_v/F_m and F'_q/F'_m are affected by environmental changes, such as nutrition and light intensity, and are directly related to the growth of algae (Misra et al., 2012; Shi et al., 2016; Wang et al., 2018). Over the past few decades, quantification of Chl*a* concentration and algal cell abundance has been extensively used to detect bloom-forming algal biomass. However, with the development of pulse amplitude modulated (PAM) fluorometry (Schreiber et al., 1986, 1997), the use of chlorophyll fluorescence parameters to estimate photosynthetic performance and stress in algae is now widespread in phytoplankton physiology both in the laboratory and field studies (Falkowski and Kolber, 1995; Higo et al., 2017; Lippemeier et al., 2001; Parkhill et al., 2001; Shen et al., 2016; Wang et al., 2014; Ma et al., 2021). For example, numerous studies have shown that in vivo fluorescence characteristics, such as F_v/F_m and F'_q/F'_m of photosystem II (PSII) are altered significantly under environmental stress in the field and algal cultures. This finding is especially pronounced in nitrogen and/or phosphorus limited scenarios suggesting that F_v/F_m and F'_q/F'_m are good proxies of algal physiological status (Geider et al., 1993; Higo et al., 2017; Lippemeier et al., 2001, 2003; Liu et al., 2011; Wang et al., 2014). On the other hand, some researches indicated that these chlorophyll fluorescence parameters can only be used as a diagnostic for unbalanced growth conditions (e.g. nutrient-starved), and further results found that F_v/F_m is not a good indicator to measure the physiological state of algae under sufficient nutrition condition (Parkhill et al., 2001; Kruskopf and Flynn, 2006; Bergmann et al., 2002; Springer et al., 2005). Moreover, the sensitivity of F_v/F_m to nutrient limitation is different among algal species (Qi et al., 2013). Further studies indicated that F_v/F_m has a species-specific response to the different growth phases (López-Sandoval et al., 2014). Therefore, it is important to explore how chlorophyll fluorescence of phytoplankton responds to various environmental stresses.

In the fluctuating growth process of algae, the variation trend of algal cell density can be characterized by oscillatory dynamics, which widely exist in nature and can be observed in many systems such as aquatic ecosystems, predator–prey systems, nervous systems, and epidemiological systems (Esmaeili et al., 2022; Chaffee and Kuske, 2011; Droop, 1983; Shen et al., 2019; Huisman et al., 2006). Photophysiology status, as an indicator of algae density change, has not been fully studied in the fluctuating growth of algae. Mathematical modeling is becoming increasingly important for describing the dynamic growth process of algae and predicting the development trend of algal blooms. Many researchers used mathematical models to study the dynamic growth process of algae and obtained significant results. Song et al. (2019) studied the effects of seasonal light intensity and nutrient availability on algae fluctuation during an algal bloom in the Bohai Sea using a stoichiometric model. Heggerud et al. (2020) used a stoichiometric model to study the specific mechanisms that drive the transient dynamics of an algal bloom. Considering the influence of environmental randomness, Zhao et al. (2020) proposed and studied a stochastic algal growth model based on the model in Song et al. (2019) and obtained the threshold conditions that determine the persistence and extinction of algae. In addition, with the development of chlorophyll fluorescence dynamics, several mechanistic models based on photosynthetic electron flow response to light have been widely applied (Eilers and Peeters, 1988; Han, 2002; García-Camacho et al., 2012; Gao et al., 2018). These mechanistic photosynthetic models can better describe the phenomenon of photoacclimation, photoinhibition and photodamage during photosynthesis (Straka and Rittmann, 2018). Some researchers used biophysical models to study the productivity of microalgae culture systems. To study the effect of photoinhibition on the productivity of algae in the runway pool culture system, Hartmann et al. (2014) proposed a model considering both photosynthesis and growth dynamics of algae. Based on the Droop-Han model (Hartmann et al., 2014), Nikolaou et al. (2016) further studied the effect of photoacclimation on algal growth by considering the kinetics of pigment synthesis. Sun et al. (2017) used a coupled biophysical model to explore the growth characteristics of *P. shikokuense* under different irradiance and phosphorus limitation scenarios. To the best of our knowledge, few studies have carried out the fluctuations in cell density and photosynthetic parameters of algae during the long-term culture process, especially for *P. shikokuense*. Therefore, this paper intends to construct a novel mathematical model based on photosynthetic parameters to describe the variation trend of algal density.

In this paper, we select *P. shikokuense*, a key bloom-forming dinoflagellate species in ECS, as the research object. We hypothesize that the growth and photosynthetic parameters of *P. shikokuense* will show a fluctuating trend in the field or batch culture, and in order to adapt to the changes of physiological processes in different growth phases, the fluctuation amplitude will gradually decrease. To test this hypothesis, we investigate the variations in bulk community values of cell abundance and its chlorophyll fluorescence parameters, such as F'_q/F'_m, α, and $rETR_{max}$ via PAM fluorometer during the outbreak of *P. shikokuense* bloom in May 2016. In addition, we estimate the same parameters for a batch culture of *P. shikokuense* over 12-time points covering a 50-day period. Moreover, to understand the relationship between algal growth and its photo-physiology status, we construct a mathematical model based on F'_q/F'_m of PSII and algal cell density. The model are calibrated based on experimental data of *P. shikokuense* and validated by the experimental data of *Symbiodinium* sp. The experimental and mathematical results provide a new insight to elucidate the mechanism of bloom formation and dissipation.

2. Materials and methods

2.1. Field sample

The field study area is found between Dongtou and Nanji Islands, located on the coast of Zhejiang Province, China (Fig. 1). According to the development of a bloom from May 9 to May 20, 2016, phytoplankton water samples were collected at a total of 57 stations. The station information, phytoplankton sample collection, species identification, and cell number counting details can be seen in our previous work (Shen et al., 2019). An aliquot of 50 ml surface seawater was separately sampled from each station to determine Chl*a* concentration, F'_q/F'_m, and rETR using the pulse amplitude modulated fluorometer (PHYTO-PAM-ED, Walz, Effeltrich, Germany) according to the previous method (Shen et al., 2019). The parameters (α and $rETR_{max}$) of the rETR vs. light curves were analyzed according to Eilers and Peeters (1988). The detection method of P_i was according to Jiang et al. (2019) with minor modification. 100 mL seawater was sampled underwater at 0.5 m and filtered by 0.45 μm cellulose acetate membrane immediately, and P_i concentration was analyzed with phosphomolybdate-blue spectrophotometry.

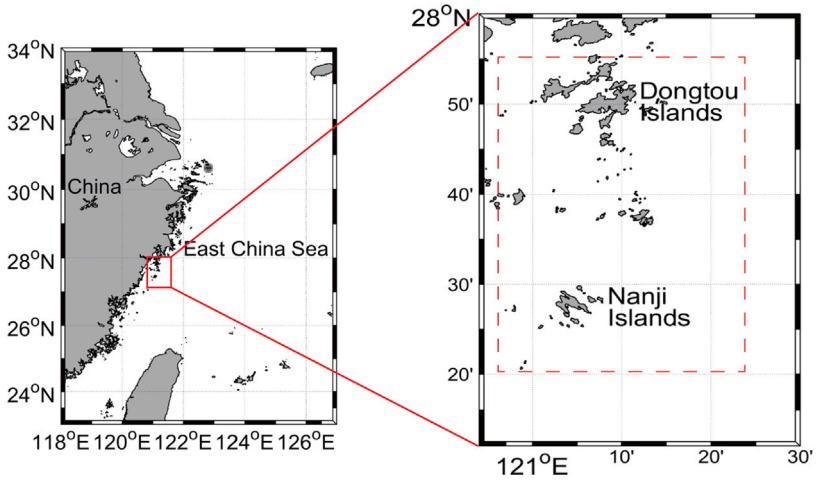

Fig. 1. The field sample investigation area in the spring of 2016 between Dongtou and Nanji Islands in the coast of Zhejiang Province (the area of the dashed frame in the right figure is the ship observation areas).

2.2. Laboratory experiment

An axenic strain of *P. shikokuense* (GY-H40) was purchased from Shanghai Guangyu Biotechnology Co., Ltd., China. The algal culture was maintained in f/2 medium (Guillard, 1975) with sterile-filtered (121 °C, 20 min, 0.45 μm Millipore membranes) seawater at a salinity of 30. The cultures ware kept at 20 ± 1 °C under a 14:10 h light-dark cycle at a photon flux of 65–70 μmol photons m^{-2} s^{-1}. The initial P_i concentration of these batch cultures is about 1.62 μM. The culture was routinely shaken twice daily until the cells reached the exponential growth phase to be used in the following experiments. All the experiments were carried out with three biological repeats.

To explore the growth status of *P. shikokuense* under long-term culture conditions, the batch cultures were grown in 600 mL of fresh f/2 media in 1000 mL flasks at an initial cell density of 7.3×10^6 cells L^{-1}. The algal culture conditions are consistent with the pre-experiments. A 0.9 mL sample was collected and preserved in 0.1 mL Lugol's solution, and 0.1 mL samples were counted in a phytoplankton counter frame (CC-F, Beijing Purity Instrument Co., Ltd., China) with an optical microscope (ECLIPSE 80i, Nikon, Japan) at 0, 2, 5, 10, 15, 20, 25, 30, 35, 40, 45, and 50 days. In addition, the determination and calculation methods of the fluorescence parameters (Chl*a*, F_q'/F_m', rETR, α, and $rETR_{max}$) and P_i concentration followed as with the field samples by synchronous sampling.

2.3. Statistical analysis

For the field sample data, due to the non-normal distribution of the data (Shapiro–Wilk test), the differences in characteristics among the sample days are analyzed using the Kruskal–Wallis test with Dunn–Bonferroni post hoc tests (IBM SPSS 22.0). For the laboratory experiment, the data are presented as the mean ± SE of triplicates, which is normally distributed and with homogeneous variance (Levene tests). Statistical differences among the sample days are analyzed using one-way ANOVA followed by Tukey's multiple range test. The generalized additive model (GAM) was used to evaluate the trend of cell abundance and fluorescence parameters over time (Fei et al., 2022; Li et al., 2019). The GAM model is constructed and calculated using the mgcv function library of the R package, and the model selection is performed using the AIC value. The relationship function adopts Gaussian distribution. The smoothing function adopts an adaptive smoothing function based on P spline, and the optimal function order is selected by automatic model simulation. In addition, generalized linear mixed model (GLMM) was used to study the relationship between cell abundance and PAM parameters (Bolker et al., 2009; Wang et al., 2018). The total phytoplankton cell density was used as the response variable. The Chl*a*, F_q'/F_m', α, and $rETR_{max}$ were used as predictor variables. Sampling sites are incorporated into the model as random effects. p values < 0.05 were considered significant. All analyses were performed using IBM SPSS Statistics 22.0 (IBM SPSS Software, Chicago, USA) and R 4.2.2, and all charts were generated using Origin Pro 2018 (OriginLab, Northampton, USA) and MATLAB (R2016b). In addition, the calculation of the dominance index (Y) is according to Sun et al. (2003).

2.4. Derivation of the model

To explore the relationship between the growth process of algae and its photo-physiology status, we propose a mathematical model to describe the interaction between the actual photochemical quantum yield of PSII (F_q'/F_m') and the cell density of algae (N). F_q'/F_m' can characterize the operational efficiency of PSII in algal cells. Under a given photosynthetically active photon flux density, this value provides a quantum yield to estimate the linear electron flux through PSII (Baker and Neil, 2008). During photosynthesis, the light energy absorbed by algal cells is mainly used for photochemical reactions and excessive excitation energy will be dissipated in the form of heat and fluorescence (García-Camacho et al., 2012). It is worth noting that photochemical reactions, heat dissipation, and chlorophyll fluorescence compete for energy consumption. The actual photochemical quantum efficiency of algal cells characterizes the ratio of energy used for photochemical reactions to total absorbed light energy. Therefore, the change of F_q'/F_m' is composed of two aspects, and the capture of light energy increases the energy available for photochemical reactions. We assume that the rate of light energy captured by algal cells is proportional to the irradiance, yielding

$$r_p = K_a I(t),$$

where K_a is the light absorption coefficient of algal cell, and $I(t)$ is the irradiance. We treat $I(t)$ as a periodic function with a light-dark cycle of 14:10 h and photon flux of 65–70 μmol photons m^{-2} s^{-1}.

With the increase of algal cell density, the specific absorption cross-section of algal cells will be reduced, thereby reducing the light capture rate of the cell (García-Camacho et al., 2012). At the same time, the absorption of light energy is also limited by the maximum actual photochemical quantum yield of algal cells. For the convenience of model expression, we use F to represent F_q'/F_m'. Therefore, the final form of light capture rate of algal cells is

$$r_p = K_a \frac{\xi}{\xi + K_1 N}\left(1 - \frac{F}{F_{max}}\right) I(t),$$

Table 1
Parameters in model (1).

Parameter	Unit	Explanation
K_a	m^2 μmol^{-1}	The light absorption coefficient of algal cell
ξ	m^2	Cellular light absorption cross-section
K_1	m^2 L $cell^{-1}$	Self-shading coefficient
F_{max}		Maximum actual quantum yield of photosystem II of algal cell
r	day^{-1}	Energy loss rate
μ_{max}	day^{-1}	Maximum growth rate of algae
K_f		Half-saturation constant for algae growth
e	day^{-1}	Death rate of algae
b	L day^{-1} $cell^{-1}$	Density limiting coefficient
τ	day	Time needed for the absorbed light energy to form new algal cells

where ξ is the cellular light absorption cross-section, K_1 is the self-shading coefficient and F_{max} is the maximum actual quantum yield of PSII of algal cells. Additionally, respiration has been long recognized as an integral part of the algae energy budget (García-Camacho et al., 2012). Therefore, energy loss due to algae respiration should be considered. We assume that the energy loss due to respiration is proportional to F and the energy loss rate is r (García-Camacho et al., 2012; Alijani et al., 2015). Thus, we arrive at the following equation for the change in the actual quantum yield

$$\frac{dF}{dt} = K_a \frac{\xi}{\xi + K_1 N}\left(1 - \frac{F}{F_{max}}\right) I(t) - rF.$$

For the process of algal growth, we use the traditional Monod equation to describe the relationship between the specific growth rate of algae (μ) and the actual photochemical quantum yield (Wang et al., 2007; Monod, 1949),

$$\mu = \mu_{max} \frac{F}{F + K_f},$$

where μ_{max} is the maximum growth rate of algae and K_f is the half-saturation constant for algal growth. Compared with the changes of photosynthetic parameters of algae, cell growth is a slow process. Therefore, the time delay τ needed for the absorption of light energy to form new cells should be considered when exploring the growth process of algal cells (García-Camacho et al., 2012). Hence, at time t, the final form of the specific growth rate of algae can be represented as

$$\mu(t) = \mu_{max} \frac{F_\tau}{F_\tau + K_f},$$

here the notation F_τ means $F(t-\tau)$. We assume that the loss of algal cells due to natural death is proportional to cell density and the natural mortality rate is e. We further assume that the loss of cell density caused by intraspecific competition is proportional to the square of cell density and the loss rate is b (Chen et al., 2015). Then the change of N can be expressed as

$$\frac{dN}{dt} = \mu_{max}\left(\frac{F_\tau}{F_\tau + K_f}\right) N - eN - bN^2.$$

According to the above formulations, we obtain a novel algal growth model.

$$\begin{cases} \dfrac{dN}{dt} = \underbrace{\mu_{max} \underbrace{\dfrac{F_\tau}{F_\tau + K_f}}_{\text{Monod equation}}}_{\mu\text{: Cell growth}} N - \underbrace{eN}_{\text{Cell death}} - \underbrace{bN^2}_{\text{Crowding loss}}, \\ \dfrac{dF}{dt} = \underbrace{K_a \dfrac{\xi}{\xi + K_1 N}\left(1 - \dfrac{F}{F_{max}}\right) I(t)}_{r_p\text{: Absorption of light energy}} - \underbrace{rF}_{\text{Energy loss due to respiration}}. \end{cases} \quad (1)$$

All parameters of the model are positive and their biological meanings are listed in Table 1.

3. Results

3.1. Fluctuation of growth during the process of P. shikokuense bloom in the field

During the investigation period, the concentration of P_i ranged from 0.06 to 2.96 μM, with an average of 0.56 μM. In the first three days (May 9, May 10, and May 12), the average values were lower than those of other days ($P < 0.05$, Fig. 2a), and the N:P ratio was about 200 (unpublished data), indicating that this investigation area was phosphorus limited. We analyzed the abundance and dominant species of phytoplankton in water samples during the investigation period (from May 9 to May 20, 2016) and that a typical *P. shikokuense* bloom occurred (the average abundance of total phytoplankton and *P. shikokuense* respectively were 6.64×10^5 cells L^{-1} and 6.59×10^5 cells L^{-1}, the dominance of *P. shikokuense* was 0.82). This bloom process can be divided into three phases: growth phase (May 9–12), maintenance phase (May 13–18) and dissipation phase (May 19–20) (Fig. 2b, (Shen et al., 2019)).

There are three troughs and two peaks during the process of this bloom in the phytoplankton abundance and perhaps more pronounced in *P. shikokuense* abundance. A similar trend is also found in Chl*a* concentration. Fig. 2b shows the fluctuation of phytoplankton abundance and Chl*a* concentration, where the values declined to the minimum values on May 12 and then increased significantly on May 13 and decreased again on May 14. It is worth noting that the substantial increase of Chl*a* and the large error bars on May 13 were due to the sharp increase in biomass at the site of NC1. The second peak was observed on May 17, and then these values declined until May 20. In addition, the total phytoplankton and *P. shikokuense* abundances are very close during the maintenance phase with a dominance of *P. shikokuense* of 0.99. In addition, we used the GAM to evaluate the trend of cell abundance and fluorescence parameters over time. The results showed that cell abundance and fluorescence parameters changed significantly with time (Fig. 4 and Table 2). As can be seen from Fig. 4, the GAM results are consistent with the ANOVA results. The total phytoplankton abundance and Chl*a* concentration had the same change trend, both experienced two peaks and finally showed a downward trend (Figs. 4a and 4d). It can be seen from the variation of the abundance of *P. shikokuense* that this bloom is obviously divided into three stages, which is consistent with the results of ANOVA (Fig. 4e).

3.2. Fluctuation of photosynthetic characteristics during the process of P. shikokuense bloom in the field

Fig. 3 and the GAM fitting results (Figs. 4b and 4c) show that the fluctuating trend of F_q'/F_m' and α is evident and consistent with that of the growth trend. The values of F_q'/F_m' and α displayed a slight increase on May 10 (0.49 and 0.194, respectively) and declined markedly on May 13. The values of F_q'/F_m' and α increased significantly again and maintained a high level in the following days (from May 14 to 18) and subsequently dropped to 0.28 and 0.119, respectively, on May 19 and increased at the end of the investigation (Figs. 3 and 4b).

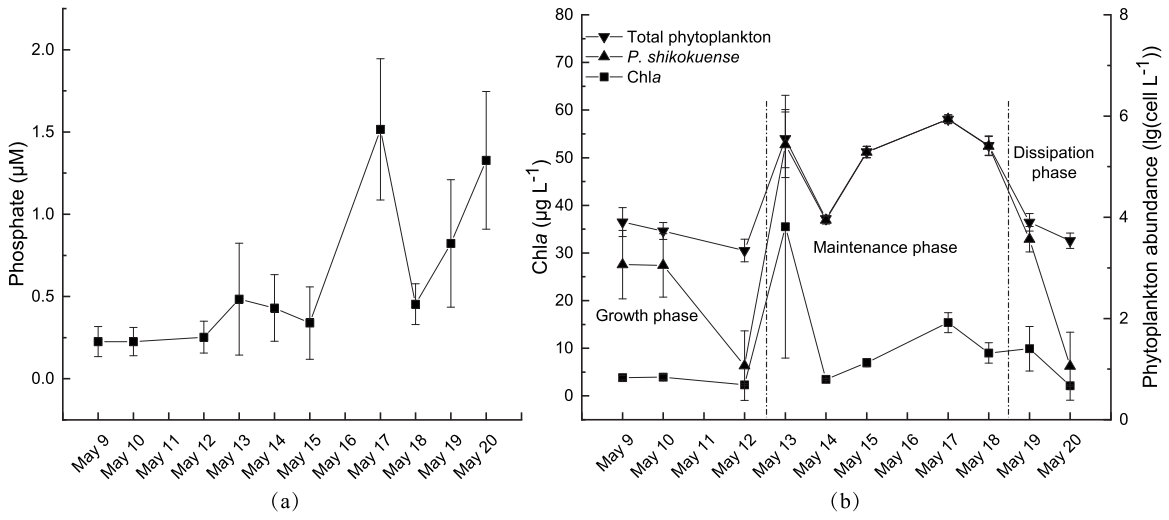

Fig. 2. Changes of phosphate concentration in the seawater (a) and algal parameters (b) including *P. shikokuense* abundance (▲), total phytoplankton abundance (▼), and Chl*a* concentration (■) during the process of *P. shikokuense* bloom in spring 2016. Data expressed as mean ± SE.

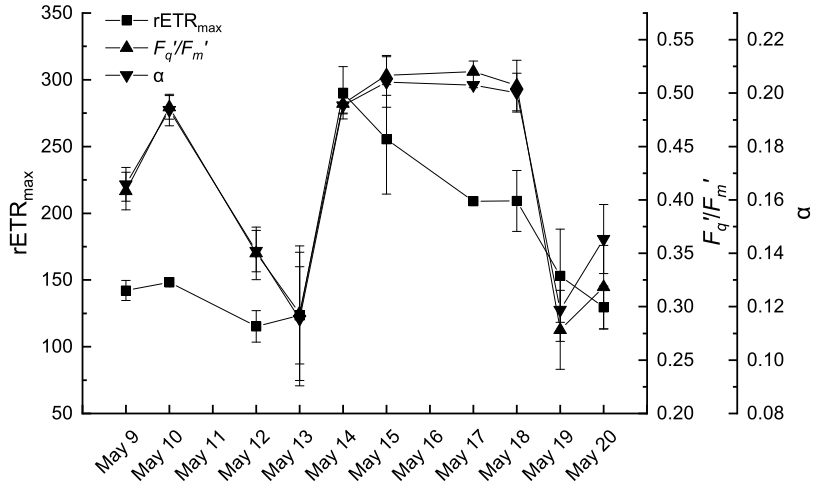

Fig. 3. Changes of $rETR_{max}$ (■), F'_q/F'_m (▲) and α(▼) during the process of *P. shikokuense* bloom in spring 2016. Data expressed as mean ± SE.

Table 2
Statistical parameters of generalized additive model.

Formula	AIC	Deviance explained (%)	R^2_{adj}	Deviance	*p*-value
ln(Total phytoplankton abundance)~ s(time)	208.96	0.7424	0.6942	80.32	$<2e^{-16}$
$\ln(F'_q/F'_m)$~ s(time)	41.49	0.4654	0.3760	4.86	0.000333
$\ln(\alpha)$ ~ s(time)	30.25	0.4661	0.3740	3.96	0.000416
ln(Chl*a*)~ s(time)	125.34	0.4713	0.3772	20.84	0.000338
ln(*P. shikokuense* abundance)~ s(time)	362.94	0.6029	0.5346	1358.11	$1.18e^{-6}$
$\ln(rETR_{max})$ ~ s(time)	75.97	0.4277	0.3336	8.94	0.00117

Table 3
Results of a GLMM to examine the association between cell abundance in the field and fluorescence parameters.

Model parameter	Coefficient (SE)	*t*-value	*p*-value
Chl*a*	0.086 (0)	1855.441	< 0.001
F'_q/F'_m	−12.99 (0.031)	−421.904	< 0.001
α	64.916 (0.095)	683.055	< 0.001
$rETR_{max}$	0.003 (0)	293.796	< 0.001

A similar trend was also observed for $rETR_{max}$ but when the values steadily declined after reaching the second peak on May 14 with a maximum of 290.3 (Figs. 3 and 4f). Comparing the results of growth and photosynthetic parameters (Figs. 2 and 3) we found that the higher the phytoplankton abundance the lower values of the photosynthetic parameters, especially in $rETR_{max}$. Furthermore, to verify the practicability of fluorescence parameters for estimating cell abundance in harmful algal blooms, we used Chl*a*, F'_q/F'_m, α, and $rETR_{max}$ fitting the GLMMs. The results showed that all tested fluorescence parameters had significant effects on cell abundance (Table 3). Therefore, these parameters may be selected to construct the model of chlorophyll fluorescence parameters and algal cell interactions.

3.3. Fluctuation of growth in P. shikokuense laboratory experiment

To aid in the characterization of the fluctuation mechanism of growth and photosynthetic parameters in the field, we performed

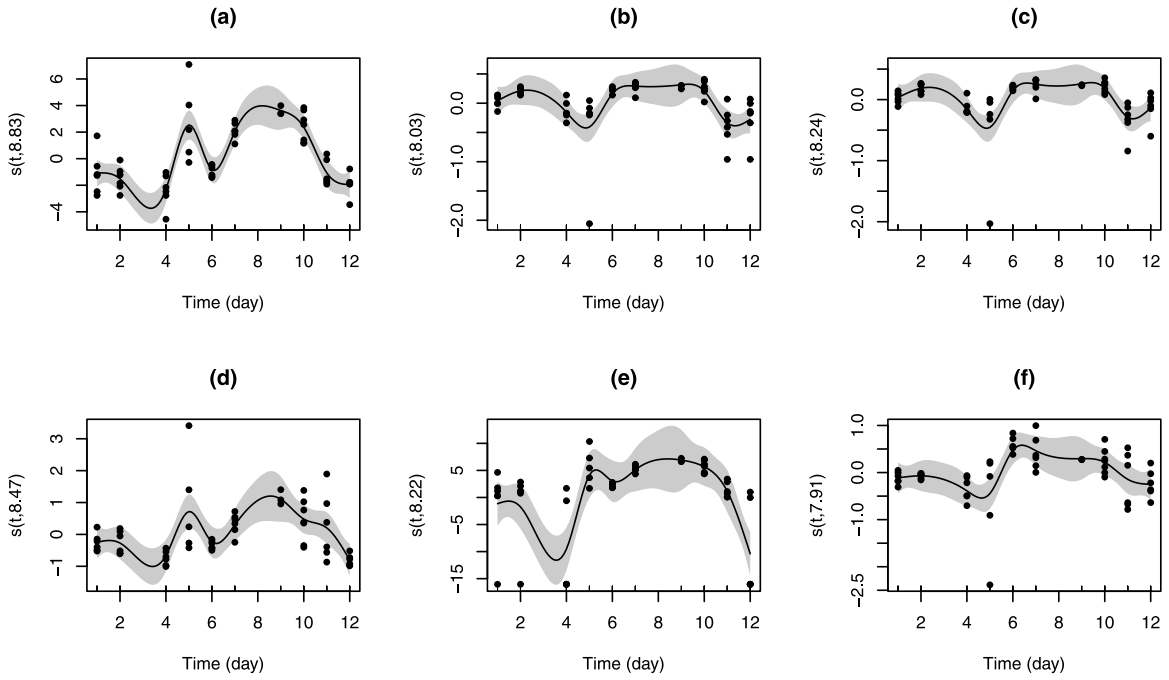

Fig. 4. Changes of cell abundance and fluorescence parameters with time in the bloom field of spring 2016. (a) Total phytoplankton abundance; (b) F'_q/F'_m; (c) α; (d) Chl*a*; (e) *P. shikokuense* abundance; (f) $rETR_{max}$; The shaded area of the trends are the 95% confidence intervals of the fitted smoothers. For simplicity, 1 to 12 are used to represent May 9 to May 20.

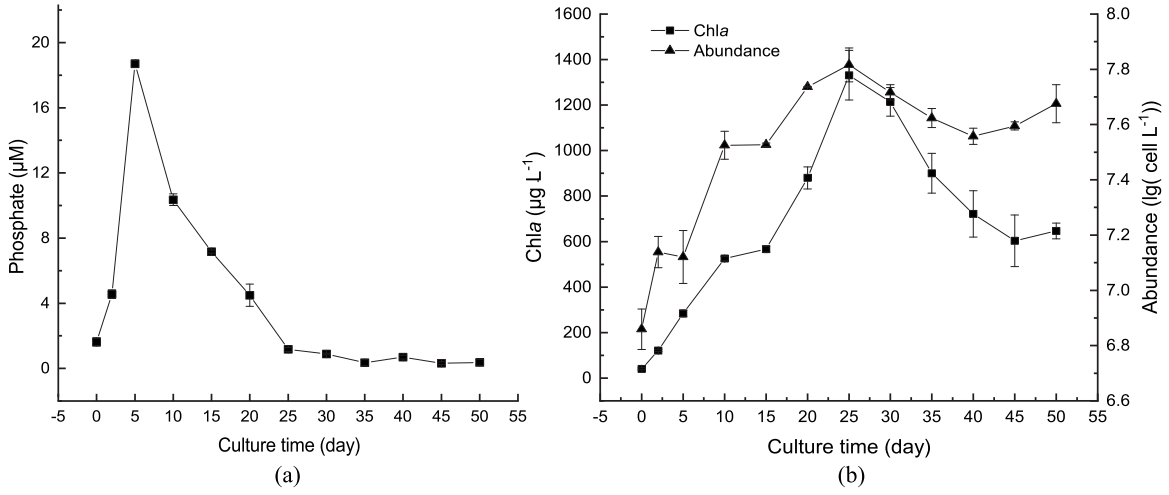

Fig. 5. (a) Changes of phosphate concentration in the medium; (b) algal parameters including *P. shikokuense* abundance (▲) and Chl*a* concentration (■) during the batch culture. Data expressed as mean ± SE.

the growth experiment for the dominant species *P. shikokuense* in the laboratory using batch culture for 50 days. In the first half of the experiment (day 0–20) the concentration of P_i was high and the values exceeded 4 μM, except for the first two days, indicating that the P_i in water is not limited. In the latter half of the experiment (day 21–50) the values of P_i were low, indicating that the *P. shikokuense* culture was under phosphorus limitation (Fig. 5a). As can be seen from Fig. 5b, *P. shikokuense* abundance and Chl*a* concentration showed an upward trend in volatility in the first 25 days and respectively obtained the maximum values of 6.67×10^7 cells L^{-1} and 1331.26 μg L^{-1} on day 25. After day 25, the values displayed a significant decrease until day 40 or 45 and then increased slightly at the end of the experiment.

3.4. Fluctuation of photosynthetic characteristics in P. shikokuense laboratory experiment

We determine the photosynthetic parameters from the same time samples as the laboratory growth experiment. Fig. 6 shows that F'_q/F'_m, α, and $rETR_{max}$ fluctuate and decrease gradually until the end of the experiment. In detail, $rETR_{max}$ increased significantly ($P < 0.05$) in the first 2 days and obtained a maximum value of 285.4 on day 2, and then decreased in the next 3 days, afterwards there were three obvious peaks on days 10, 25 and 35 and finally reached a minimum value of 7.6 at the end of the experiment. Similar trends were observed in the other two parameters, only the fluctuation amplitude of F'_q/F'_m and α

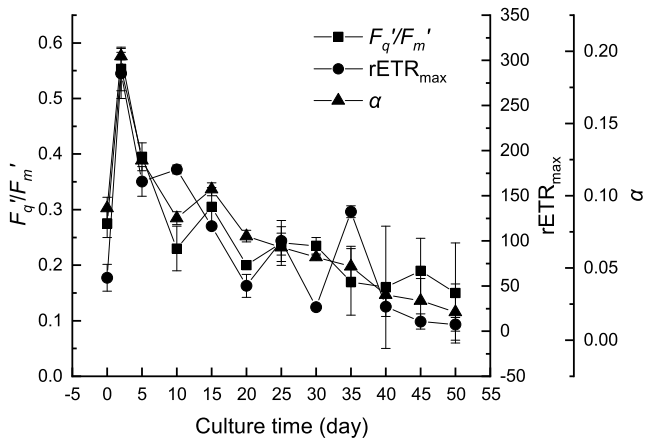

Fig. 6. Changes of F_q'/F_m' (■), rETR$_{max}$ (•) and α(▲) during the batch culture. Data expressed as mean ± SE.

Table 4
Parameter values of model (1) estimated from experimental data of F_q'/F_m' and N in *P. shikokuense*.

Parameter	Unit	Value
K_a	m^2 μmol^{-1}	1.124×10^{-3}
ξ	m^2	1.8×10^{-12}
K_1	m^2 L cell^{-1}	2.8553×10^{-15}
F_{max}		0.9
r	day^{-1}	0.23
μ_{max}	day^{-1}	0.76
K_f		0.52
e	day^{-1}	0.175
b	L day^{-1} cell^{-1}	6.8×10^{-10}
τ	day	4.8

is not as prominent as that of rETR$_{max}$ in the middle and later parts of the experiment.

3.5. Experimental data fitting

Model (1) is calibrated based on the experimental data of *P. shikokuense* using the least square method and is implemented by the function "fmincon" in MATLAB R2016b. The model fitting results and parameter values are shown in Fig. 7 and Table 4, respectively. In addition, the model cost and relative error are calculated using the method in Gao et al. (2022). Fig. 7 shows that the fitted curve of model (1) fits the experimental data of N well, with the model cost of 0.632 and relative error of −1.1707. For F_q'/F_m', the model fits the overall trend of the experimental data well, especially the first peak and the last 15 days. The corresponding model cost and relative error are 0.9336 and −2.1483, respectively. It is worth noting that the simulation curve has a small wave trend, which indicates that the model can reproduce the diurnal periodic changes of algae photosynthesis. In addition, the model was validated by the experimental data of *Symbiodinium* sp. The initial cell density and phosphate concentration are 4.74 × 10^6 cells L^{-1} and 2.74 μM, respectively. During the experiment, the cultures were kept at a 12:12 h light-dark cycle with the photon flux of 50 μmol photons m^{-2} s^{-1}. The other culture conditions are the same as in Section 2.2. Fig. 8 shows a comparison between our simulation and experiment data. The variations of cell density and actual quantum yield are shown in Fig. 8(a) and 8(b). It can be seen from the fitting results that the experimental data of *Symbiodinium* sp. can be well fitted by the trained model, here the model parameter values from in Table 4 only changed the irradiance $I(t)$ and energy loss rate r. Combined with the calibration and validation results, it shows that the model can well describe the interaction between photosynthetic parameters and cell density during algae growth.

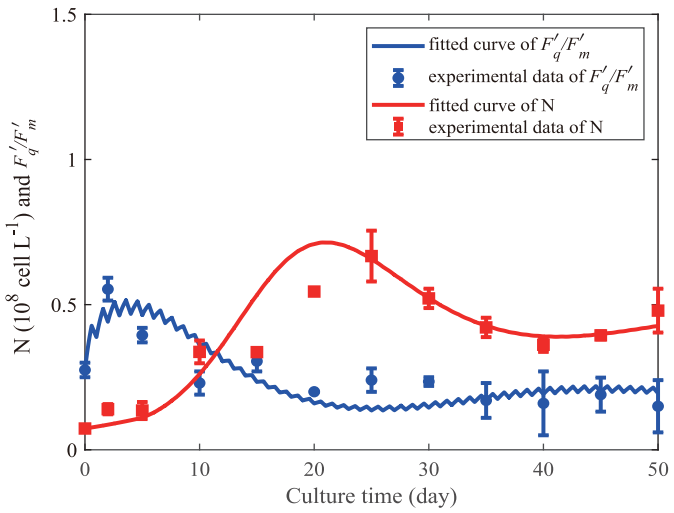

Fig. 7. Experimental data and the fitted curve of model (1) for F_q'/F_m' and N of *P. shikokuense*. The parameters K_a, K_1, F_{max}, K_f, r, μ_{max}, b, e and τ in model (1) are estimated by fitting the two data sets of F_q'/F_m' and N at the same time. Data expressed as mean ± SE.

3.6. Sensitivity analysis

To provide a comprehensive understanding of the influence of the change of parameter values on the results of the model, we perform a sensitivity analysis. Here, the sensitivity system given by the partial derivatives of variables $X = \{N, F\}$ of the model (1) is derived with respect to the parameters $q = \{K_a, \mu_{max}, e, b, K_1, F_{max}, K_f, r\}$ (the detail methods please see Bortz and Nelson (2004), Sourav et al. (2020)). The parameter's baseline values are from Table 4. The logarithmic sensitivity curves ($\frac{\partial X}{\partial q}\frac{q}{X}$) for all variables of model (1) are displayed in Fig. 9. From the logarithmic sensitivity solution curve, the dynamic response of the model solution to parameter changes at different times can be obtained. In addition, we can also get the percentage change of the model solution caused when that parameter is doubled. As can be seen from Fig. 9, the logarithmic sensitivity solution of all parameter show a fluctuation state in the early time and eventually reaches a steady state. From the results of sensitivity analysis, the maximum growth rate (μ_{max}), the light absorption coefficient (K_a), and the maximum actual quantum yield of photosystem II (F_{max}) have positive effects on the algal density, and the other parameters have negative effects. Here, μ_{max} has the largest positive effect on cell density, and e has the largest negative effect. In contrast, μ_{max} has the most negative effect on the actual quantum yield, and e has the most positive effect. This may be due to the self-shading effect. As the density of algae increases, the light energy captured by individual algae cells decreases, so μ_{max} has a negative effect. It is worth noting that the logarithmic sensitivity solutions with respect to K_1 and r tend to the same steady-state values over time, indicating that the two parameters have similar effects on cell density and actual quantum yield when the system is stable. Interestingly, K_a has a positive effect on cell density and b has a negative effect, both of them have a positive effect on actual quantum yield, and the effects of the two parameters on actual quantum yield are similar when the system reaches a steady state.

4. Discussion

This study exhibits the first attempt to compare the growth and photosynthetic parameters of a *P. shikokuense* bloom/batch culture at different time points throughout a bloom process/growth cycle. We aim to test the hypothesis that the values of algal abundance and photosynthetic parameters would fluctuate to suit the changes of

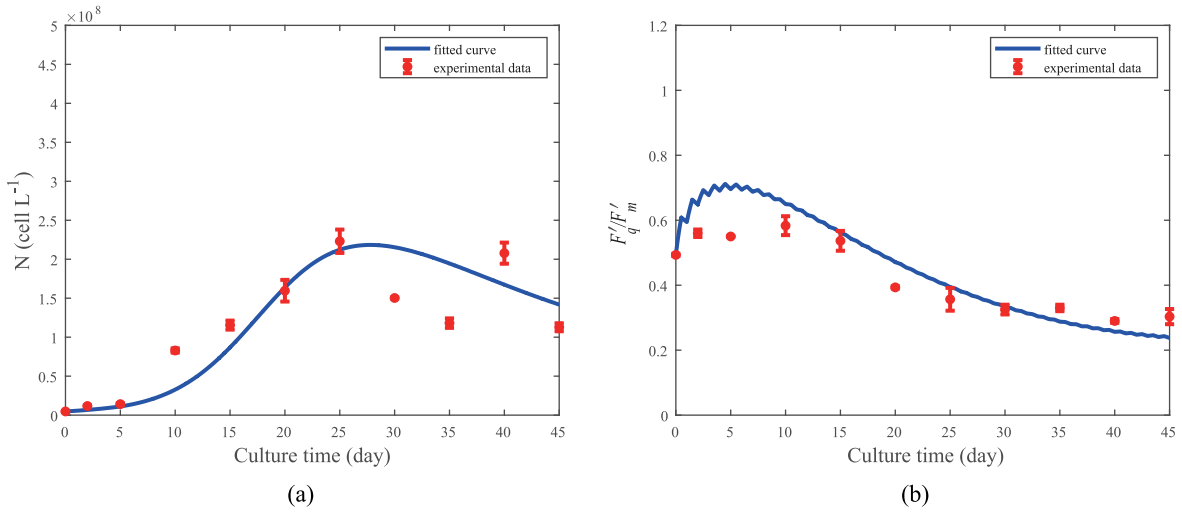

Fig. 8. Model validation using the data of *Symbiodinium* sp. under the condition of P_i replete at 20 °C. (a) cell density; (b) actual quantum yield. Here $I(t)$ is a periodic function with a light-dark cycle of 12:12 h and photon flux of 50 μmol photons m^{-2} s^{-1}, $r = 0.046$ and the rest parameter values are from Table 4. Data expressed as mean ± SE.

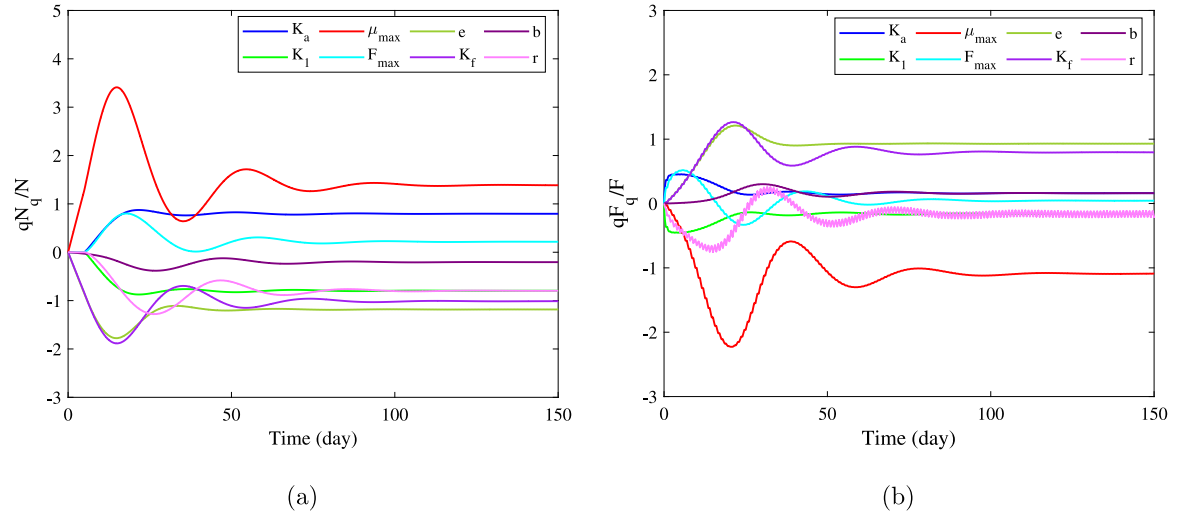

Fig. 9. The logarithmic sensitivity solutions ($\frac{\partial X}{\partial q}\frac{q}{X}$) for both variables of model (1), with respect to the model parameters. The parameter values are shown in Table 4.

intracellular biological processes. These experimental results indicate that the growth and photosynthetic parameters of *P. shikokuense* show a fluctuating phenomenon and that the photosynthetic parameters have a faster response than growth parameters. According to the results of GLMMs fitted by photosynthetic parameters and cell abundance, these photosynthetic parameters have significant effects on cell abundance. Therefore, using the actual quantum yield and cell density as the research variables, we proposed a novel algal growth model incorporating cell growth delay. Then, the model was calibrated by the long-term experimental data of *P. shikokuense* and validated by the experimental data of *Symbiodinium* sp. Based on the model calibration and verification results, the model can better describe the interaction between cell density and photosynthetic parameters during the growth of algae. It is worth noting that, unlike the statistical model, our model is a delay differential equation. For the parameterized model, when the initial value of variables is given, the model has a unique solution curve. Therefore, the model can predict the growth of algae based on the relevant data before the occurrence of HABs, and provide new insight for the early warning of HABs combined with the critical threshold of biomass when HABs occurs.

4.1. Fluctuation of growth and photosynthetic characteristics P. shikokuense bloom in the field

Many studies have begun to focus on the application of PAM technology to *in situ* determination of chlorophyll fluorescence parameters to assess the photosynthetic physiological status of algae during the blooming process rather than to record the changes of algal abundance merely. For example, some researches indicated that changes in photosynthetic characteristics (e.g. F_v/F_m) could be a good indicator of algal bloom formation and succession in the field (Higo et al., 2017; Wang et al., 2014). On the contrary, Springer et al. (2005) found that the values of F_v/F_m were consistently 0.6–0.8 during the bloom, providing little evidence of photo-physiological stress, as would have been expected under nutrient-limiting conditions. The reason for these two different results may be due to differences in measurement systems and sampling intervals or differences in species growth status (Higo et al., 2017; Springer et al., 2005; Wang et al., 2014; Parkhill et al., 2001). An additional mechanism was shown in detail by Parkhill et al. (2001), who indicated that F_v/F_m is not a robust diagnostic for all nutrient-stressed conditions because variable fluorescence can only be used as a diagnostic for nutrient-starved unbalanced growth conditions. To further examine this possibility, we take daily sampling to limit

the differences of measurement. The GLMMs results showed that the variable chlorophyll fluorescence parameters are closely related to the abundance of algae (Table 3) and the presence of a time-lag phenomenon (Figs. 2b and 3). In addition, our investigation results showed that the concentration of P_i was deficient during the *P. shikokuense* bloom (Fig. 2a). It is shown that the water body is in a phosphorus limited state when the dinoflagellate blooms occur, but it is very difficult to determine whether algal cells are in unbalanced growth conditions during this stage (later spring to early summer). Therefore, we speculate that whether or not P_i is acting as a stressor on algal cells may be more closely related to the photo-physiological status. Furthermore, the concentration of intracellular P_i (the total cellular P_i including the intracellular P_i and surface-adsorbed P_i where latter may account for 15% to 45% of total cellular P_i in the different phases of blooms (Sañudo-Wilhelmy et al., 2004)) can be used as a good indicator to measure whether algal cells are under phosphorus stress. Our previous study found that intracellular P_i is important to algal growth (Jiang et al., 2019; Gao et al., 2022) and the photosynthetic phosphorylation level, Calvin cycle efficiency, photosynthetic rate, and block recycling of NADP and NADPH will be inhibited by this limitation (Fredeen et al., 1990). Therefore, further investigation of the exact mechanisms involved in intracellular P_i and photo-physiological parameters in the field is needed.

4.2. Fluctuation of growth and photosynthetic characteristics P. shikokuense in the laboratory

Phosphorus is considered to be a common limiting factor for the growth of phytoplankton especially when blooms occur (Huang et al., 2007). In this study, phosphorus limitation clearly affected cell abundance and Chl*a* concentration after 25 days of culturing compared with the first 20 days in phosphorus sufficient conditions (Fig. 5). During the experiment, the concentration of P_i was low in the first 2 days because the culture of *P. shikokuense* was in a phosphorus starvation state (the value of alkaline phosphatase was about 14000 fmol $cell^{-1}$ h^{-1}, unpublished data) and a lot of P_i were quickly absorbed in the cell surface, a similar result was observed in our previous studies (Jiang et al., 2019). However, excessive P_i was released into the water because it could not be absorbed and utilized before being exuded. The concentration of P_i increased on day 5 with a maximum value of 18.70 μM in the medium. Although the P_i concentration in the medium was low after the 20th day, the algae continued to grow rapidly, and the abundance and Chl*a* concentration continued to increase and began to decrease after 5 days (Fig. 5). During the experiment, from day 25 to day 40, the algal abundance decreased significantly, followed by the values increasing again until the end of the experiment. This has also been observed in other studies, such as *Alexandium minutum* (Lippemeier et al., 2003), *Thalassirosira weissflogii* (Liu et al., 2011). In addition, there was a small fluctuation of *P. shikokuense* abundance in the first 25 days (in P_i sufficient conditions) followed by a large fluctuation in the later 25 days (in P_i deficient condition). By comparison, chlorophyll fluorescence parameters have a faster response than that of algal growth during the experiment (Fig. 6). Furthermore, there were obvious fluctuations in *P. shikokuense* abundance and photosynthetic characteristics.

In particular, we see fluctuations in $rETR_{max}$ which clearly identified algal photo-physiological status under different nutrient conditions. Although there are differing opinions about the use of these parameters as indicators for algal blooms under various environmental stressors (Kruskopf and Flynn, 2006; Lippemeier et al., 2001; Liu et al., 2011; Parkhill et al., 2001), this study showed a clear time delay relationship between the photosynthetic characteristics and the abundance of *P. shikokuense* under various degrees of phosphorus limitation. With the extension of culture time, the concentration of P_i decreased to a very low level in the last 25 days (Fig. 5a), indicating the cultures were under phosphorus limitation. Note that *P. shikokuense* was not under nitrogen limitation because the growth of *P. shikokuense* has little demand for nitrogen, especially on nitrate, which had concentrations still above 37 μM after 33 days of culture when the initial nutrient was at a f/2 level (Shen and Li, 2016). The values of F_q'/F_m', α, and $rETR_{max}$ fluctuated and decreased to 0.15, 0.032, and 7.55, respectively, at the end of the experiment (Fig. 6). Similar results have been observed in the harmful Raphidophyte *Chattonella antiqua* reported by Qiu et al. (2013) where they conducted the complete growth cycle culture experiment under different nutrient conditions. The control group's results showed the F_v/F_m value changes; from 0.58 to 0.70 during the exponential phase, from 0.16 to 0.55 during the stationary phase with some fluctuations, and increased slightly during the decline phase. The relative pattern of variation in F_v/F_m in the nutrient-limited group was similar to the control group. There were many reasons for the fluctuation of photosynthetic parameters during the long time culture. Some studies suggested that the value of F_v/F_m was overestimated because of the presence of photosynthetically non-functional (dead) cells and cell detritus (Franklin et al., 2009). However, there is strong evidence that photosynthetic parameter values of some algae decrease under phosphorus stress (Liu et al., 2011; Qi et al., 2013) and increase immediately after being supplemented (Lippemeier et al., 2001, 2003). Therefore, we believe that photosynthetic parameter values are the key to understanding whether the intracellular P_i of algae is in a limited state.

4.3. Model fitting of experimental data of P. shikokuense

In this paper, we establish a novel algal growth model incorporating growth delay based on the interaction between the actual quantum efficiency of photosynthesis and algal growth. Intuitive fitting results, model cost, and relative error show that the model can reproduce the changes in cell abundance and photo-physiology status during *P. shikokuense* culture. It is worth noting that this model coupled the photo-physiology status and growth state of algae, which is similar to the models of Hartmann et al. (2014) and Nikolaou et al. (2016). Compared with the models of Hartmann et al. (2014) and Nikolaou et al. (2016), our model is simpler and has fewer free parameters. Our model can directly describe the change of cell density based on the photosynthetic parameters of algae, which makes the measurement of experimental data of model variables simpler and more convenient for model verification. In addition, the time delay between algal growth status and photo-physiology status was incorporated. This model can simulate the phenomenon of fluctuation of cell density and photo-physiology status in the process of *P. shikokuense* culture. During the whole culture period, the experimental data and the fitted curve of the model show a trend of large oscillatory variation (Fig. 7), which may be caused by the delay between the slow growth of algae and the rapid change of photo-physiology status. The time delay may cause the system to lose stability, and oscillation may occur when there is a phase change between the received signal and the response to the signal (Droop, 1983; Mackey and Glass, 1977; Misra et al., 2020; An et al., 2019). Melendez-Alvarez et al. (2021) found that the feedback mechanism of cell growth can lead to the fluctuation of cell density through a molecular mathematical model combined with experimental data.

In this model, we only consider the effect of the photo-physiology status of algae on cell growth, while the effect of limited nutrients (e.g., phosphorus) was ignored. Phosphorus plays an important role in the photosynthesis of phytoplankton, such as the Calvin cycle and regulation of some enzyme activity (Wang et al., 2004; Shen and Li, 2016). An interesting avenue of future work would be to incorporate the effects of phosphorus on algal growth and photo-physiology status into the model. An ecological stoichiometry model is a powerful tool for combining energy balance with various of nutrients in an ecosystem. Models based on ecological stoichiometry have been widely used to explore various ecological mechanisms, such as predator–prey systems, algae-daphnia interactions, and nutrient uptake processes in

phytoplankton (Peace and Wang, 2019; Yuan et al., 2020; Davies and Wang, 2021; Yan et al., 2021; Zhang et al., 2021; Heggerud et al., 2020). To describe the growth characteristics of algae more accurately, the influence of limiting nutrients on algal growth can be further considered based on the model proposed in this paper combined with stoichiometric mechanisms. López-Sandoval et al. (2014) have shown that the size of the cell can affect the metabolic rate of the species. For example, the relationship between photosynthesis and cell size is unimodal, with the highest rate measured in medium-sized species. Therefore, our model is unlikely to be applied to all algae species. We need to combine the actual data to adjust the relevant model parameters according to the species specificity, in order to be suitable for other HABs species. In addition, we speculate that for species with close taxonomic status (such as species of the same family or genus), the applicability of the model is better due to the similarity of their ecological characteristics. We validate the model with the data of *Symbiodinium* sp. and obtain good fitting results. One possible reason is that *P. shikokuense* and *Symbiodinium* sp. have similar taxonomic status. In general, combined with marine field data, the established prediction model for specific phytoplankton species will help to effectively predict the outbreak of harmful algal blooms.

Funding

This work was supported by the National Natural Science Foundation of China (grant numbers 11671260; 12071293; 41506194); the Natural Sciences and Engineering Research Council of Canada (grant numbers RGPIN-2020-03911, RGPAS-2020-00090).

CRediT authorship contribution statement

Anglu Shen: Conducted the experimental work, Conducted and analysis data, Wrote the first draft. **Shufei Gao:** Conducted and analysis data, Wrote the first draft. **Christopher M. Heggerud:** Commented and amended on the manuscript. **Hao Wang:** Designed this study, Commented and amended on the manuscript. **Zengling Ma:** Commented and amended on the manuscript. **Sanling Yuan:** Designed this study, Commented and amended on the manuscript.

Declaration of competing interest

The authors declare that they have no known competing financial interests or personal relationships that could have appeared to influence the work reported in this paper.

Data availability

All data used in this study can be found in the manuscript and its supplementary materials.

Appendix A. Supplementary data

Supplementary material related to this article can be found online at https://doi.org/10.1016/j.ecolmodel.2023.110310.

References

Alijani, M.K., Wang, H., Elser, J.J., 2015. Modeling the bacterial contribution to planktonic community respiration in the regulation of solar energy and nutrient availability. Ecol. Complex. 23, 25–33. http://dx.doi.org/10.1016/j.ecocom.2015.05.002.

An, Q., Beretta, E., Kuang, Y., Wang, C.C., Wang, H., 2019. Geometric stability switch criteria in delay differential equations with two delays and delay dependent parameters. J. Differential Equations 266, 7073–7100. http://dx.doi.org/10.1016/j.jde.2018.11.025.

Baker, Neil, R., 2008. Chlorophyll fluorescence: a probe of photosynthesis in vivo. Annu. Rev. Plant. Biol. 59, 89. http://dx.doi.org/10.1146/annurev.arplant.59.032607.092759.

Bergmann, T., Richardson, T.L., Paerl, H.W., Pinckney, J.L., Schofield, O., 2002. Synergy of light and nutrients on the photosynthetic efficiency of phytoplankton populations from the Neuse River Estuary, North Carolina. J. Plankton Res. 24, 923–933. http://dx.doi.org/10.1093/plankt/24.9.923.

Bolker, B.M., Brooks, M.E., Clark, C.J., Geange, S.W., Poulsen, J.R., Stevens, M.H.H., White, J.S.S., 2009. Generalized linear mixed models: a practical guide for ecology and evolution. Trends Ecol. Evol. 24, 127–135. http://dx.doi.org/10.1016/j.tree.2008.10.008.

Bortz, D.M., Nelson, P.W., 2004. Sensitivity analysis of a nonlinear lumped parameter model of HIV infection dynamics. Bull. Math. Biol. 66, 1009–1026. http://dx.doi.org/10.1016/j.bulm.2003.10.011.

Chaffee, J., Kuske, R., 2011. The effect of loss of immunity on noise-induced sustained oscillations in epidemics. Bull. Math. Biol. 73, 2552–2574. http://dx.doi.org/10.1007/s11538-011-9635-7.

Chai, Z.Y., Wang, H., Deng, Y.Y., Hu, Z.X., Tang, Y.Z., 2020. Harmful algal blooms significantly reduce the resource use efficiency in a coastal plankton community. Sci. Total Environ. 704, 135381. http://dx.doi.org/10.1016/j.scitotenv.2019.135381.

Chen, N.S., Chen, Y., 2021. Advances in the study of biodiversity of phytoplankton and red tide species in China (II):The East China Sea. Oceanologia Et Limnologia Sinica 52, 363–418, (in Chinese with English abstract).

Chen, M., Fan, M., Liu, R., Wang, X.Y., Yuan, X., Zhu, H.P., 2015. The dynamics of temperature and light on the growth of phytoplankton. J. Theoret. Biol. 385, 8–19. http://dx.doi.org/10.1016/j.jtbi.2015.07.039.

Chen, T.T., Liu, Y., Xu, S., Song, S.Q., Li, C.W., 2020. Variation of *Amoebophrya* community during bloom of *Prorocentrum donghaiense* Lu in coastal waters of the East China Sea. Estuar. Coast. Shelf S. 243, 106887. http://dx.doi.org/10.1016/j.ecss.2020.106887.

Davies, C.M., Wang, H., 2021. Contrasting stoichiometric dynamics in terrestrial and aquatic grazer–producer systems. J. Biol. Dyn. 15, S3–S34. http://dx.doi.org/10.1080/17513758.2020.1771442.

Diaz, J., Ingall, E., Benitez-Nelson, C., Paterson, D., de Jonge, M.D., McNulty, I., Brandes, J.A., 2008. Marine polyphosphate: a key player in geologic phosphorus sequestration. Science 320, 652–655. http://dx.doi.org/10.1126/science.1151751.

Droop, M., 1983. 25 Years of algal growth kinetics a personal view. Bot. Mar. 26, 99–112. http://dx.doi.org/10.1515/botm.1983.26.3.99.

Eilers, P.H.C., Peeters, J.C.H., 1988. A model for the relationship between light intensity and the rate of photosynthesis in phytoplankton. Ecol. Model. 42, 199–215. http://dx.doi.org/10.1016/0304-3800(88)90057-9.

Esmaeili, S., Hastings, A., Abbott, K., Machta, J., Nareddy, V., 2022. Noise-induced versus intrinsic oscillation in ecological systems. Ecol. Lett. 25, 814–827. http://dx.doi.org/10.1111/ele.13956.

Falkowski, P.G., Kolber, Z., 1995. Variations in chlorophyll fluorescence yields in phytoplankton in the world oceans. Funct. Plant Biol. 22, 341–355. http://dx.doi.org/10.1071/pp9950341.

Fei, Y.J., Yang, S.L., Fan, W., Shi, H.M., Zhang, H., Yuan, S.L., 2022. Article relationship between the spatial and temporal distribution of squid-jigging vessels operations and marine environment in the North Pacific Ocean. J. Mar. Sci. Eng. 10, 550. http://dx.doi.org/10.3390/jmse10040550.

Franklin, D.J., Choi, C.J., Hughes, C., Malin, G., Berges, J.A., 2009. Effect of dead phytoplankton cells on the apparent efficiency of photosystem II. Mar. Ecol. Prog. Ser. 382, 35–40. http://dx.doi.org/10.3354/meps07967.

Fredeen, A.L., Raab, T.K., Rao, I.M., Terry, N., 1990. Effects of phosphorus nutrition on photosynthesis in *Glycine max* (L.) Merr.. Planta 181, 399–405. http://dx.doi.org/10.1007/BF00195894.

Gao, X., Bo, K., Dennis, V.R., 2018. Simulation of algal photobioreactors: recent developments and challenges. Biotechnol. Lett. 40, http://dx.doi.org/10.1007/s10529-018-2595-3.

Gao, S.F., Shen, A.L., Jiang, J., Wang, H., Yuan, S.L., 2022. Kinetics of phosphate uptake in the dinoflagellate *Karenia mikimotoi* in response to phosphate stress and temperature. Ecol. Model. 468, 109909. http://dx.doi.org/10.1016/j.ecolmodel.2022.109909.

García-Camacho, F., Sánchez-Mirn, A., Molina-Grima, E., Camacho-Rubio, F., Merchuck, J.C., 2012. A mechanistic model of photosynthesis in microalgae including photoacclimation dynamics. J. Theoret. Biol. 304, 1–15. http://dx.doi.org/10.1016/j.jtbi.2012.03.021.

Geider, R.J., La Roche, J., Greene, R.M., Olaizola, M., 1993. Response of the photosynthetic apparatus of *Phaeodactylum tricornutum* (Bacillariophyceae) to nitrate, phosphate, or iron starvation. J. Phycol. 29, 755–766. http://dx.doi.org/10.1111/j.0022-3646.1993.00755.x.

Gómez, F., Zhang, H., Rosellt, L., Lin, S.J., 2021. Detection of *Prorocentrum shikokuense* in the Mediterranean Sea and evidence that *P. dentatum*, *P. obtusidens* and *P. shikokuense* are three different species (Prorocentrales, Dinophyceae). Acta Protozool. 60, 47–59. http://dx.doi.org/10.4467/16890027AP.21.006.15380.

Guillard, R.R.L., 1975. Culture of phytoplankton for feeding marine invertebrates. In: Culture of Marine Invertebrate Animals. Springer, pp. 29–60. http://dx.doi.org/10.1007/978-1-4615-8714-9_3.

Han, B.P., 2002. A mechanistic model of algal photoinhibition induced by photodamage to photosystem-II. J. Theoret. Biol. 214, 519–527. http://dx.doi.org/10.1006/jtbi.2001.2468.

Hartmann, P., Béchet, Q., Bernard, O., 2014. The effect of photosynthesis time scales on microalgae productivity. Bioproc. Biosyst. Eng. 37, 17–25. http://dx.doi.org/10.1007/s00449-013-1031-2.

Heggerud, C.M., Wang, H., Lewis, M.A., 2020. Transient dynamics of a stoichiometric cyanobacteria model via multiple-scale analysis. SIAM J. Appl. Math. 80, 1223–1246. http://dx.doi.org/10.1137/19M1251217.

Higo, S., Yamatogi, T., Ishida, N., Hirae, S., Koike, K., 2017. Application of a pulse-amplitude-modulation (PAM) fluorometer reveals its usefulness and robustness in the prediction of *Karenia mikimotoi* blooms: A case study in Sasebo Bay, Nagasaki, Japan. Harmful Algae 61, 63–70. http://dx.doi.org/10.1016/j.hal.2016.11.013.

Hou, J.J., Huang, B.Q., Cao, Z.R., Chen, J.X., Hong, H.S., 2007. Effects of nutrient limitation on pigments in thalassiosira weissflogii and prorocentrum donghaiense. J. Integrat. Plant Biol. 49, 12. http://dx.doi.org/10.1111/j.1744-7909.2007.00449.x.

Huang, B.Q., Ou, L.J., Wang, X.L., Huo, W.Y., Li, R.X., Hong, H.S., Zhu, M.Y., Qi, Y.Z., 2007. Alkaline phosphatase activity of phytoplankton in East China Sea coastal waters with frequent harmful algal bloom occurrences. Aquat. Microb. Ecol. 49, 195–206. http://dx.doi.org/10.3354/ame01135.

Huisman, J., Thi, N., Karl, D.M., Sommeijer, B., 2006. Reduced mixing generates oscillations and chaos in the oceanic deep chlorophyll maximum. Nature 439, 322–325. http://dx.doi.org/10.1038/NATURE04245.

Jiang, J., Shen, A.L., Wang, H., Yuan, S.L., 2019. Regulation of phosphate uptake kinetics in the bloom-forming dinoflagellates *Prorocentrum donghaiense* with emphasis on two-stage dynamic process. J. Theoret. Biol. 463, 12–21. http://dx.doi.org/10.1016/j.jtbi.2018.12.011.

Kong, F.Z., Xu, Z.J., Yu, R., Yuan, Y.Q., Zhou, M.J., 2016. Distribution patterns of phytoplankton in the Changjiang River estuary and adjacent waters in spring 2009. Chin. J. Oceanol. Limn. 34, 902–914. http://dx.doi.org/10.1007/s00343-016-4202-6.

Kruskopf, M., Flynn, K.J., 2006. Chlorophyll content and fluorescence responses cannot be used to gauge reliably phytoplankton biomass, nutrient status or growth rate. New Phytol. 169, 525–536. http://dx.doi.org/10.2307/3694692.

Kustka, A., Sañudo-Wilhelmy, S., Carpenter, E.J., Capone, D.G., Raven, J.A., 2003. A revised estimate of the iron use efficiency of nitrogen fixation, with special reference to the marine cyanobacterium *Trichodesmium* spp.(Cyanophyta). J. Phycol. 39, 12–25. http://dx.doi.org/10.1046/j.1529-8817.2003.01156.x.

Li, R., Xu, L., Bjornstad, O., Liu, K., Song, T., Chen, A., Xu, B., Liu, Q., Stenseth, N.C., 2019. Climate-driven variation in mosquito density predicts the spatiotemporal dynamics of dengue. Proc. Natl. Acad. Sci. USA 116, 201806094. http://dx.doi.org/10.1073/pnas.1806094116.

Lin, J.N., Yan, T., Zhang, Q.C., Wang, Y.F., Liu, Q., Zhou, M.J., 2014. In situ detrimental impacts of *Prorocentrum donghaiense* blooms on zooplankton in the East China Sea. Mar. Pollut. Bull. 88, 302–310. http://dx.doi.org/10.1016/j.marpolbul.2014.08.026.

Lippemeier, S., Frampton, D.M.F., Blackburn, S.I., Geier, S.C., Negri, A.P., 2003. Influence of phosphorus limitation on toxicity and photosynthesis of *Alexandrium minutum* (dinophyceae) monitored by in-line detection of variable chlorophyll fluorescence. J. Phycol. 39, 320–331. http://dx.doi.org/10.1046/j.1529-8817.2003.01019.x.

Lippemeier, S., Hintze, R., Vanselow, K., Hartig, P., Colijn, F., 2001. In-line recording of PAM fluorescence of phytoplankton cultures as a new tool for studying effects of fluctuating nutrient supply on photosynthesis. Eu. J. Phycol. 36, 89–100. http://dx.doi.org/10.1080/09670260110001735238.

Liu, S., Guo, Z.L., Li, T., Huang, H., Lin, S.J., 2011. Photosynthetic efficiency, cell volume, and elemental stoichiometric ratios in *Thalassirosira weissflogii* under phosphorus limitation. Chin. J. Oceanol. Limn. 29, 1048. http://dx.doi.org/10.1007/s00343-011-0224-2.

López-Sandoval, D.C., Rodríguez-Ramos, T., Cermeño, P., Sobrino, C., Marañón, E., 2014. Photosynthesis and respiration in marine phytoplankton: relationship with cell size, taxonomic affiliation, and growth phase. J. Exp. Mar. Biol. Ecol. 457, 151–159. http://dx.doi.org/10.1016/j.jembe.2014.04.013.

Lu, S.H., Ou, L.J., Dai, X.F., Cui, L., Dong, Y.L., Wang, P.B., Li, D.M., Lu, D.D., 2022. An overview of *Prorocentrum donghaiense* blooms in China: Species identification, occurrences, ecological consequences, and factors regulating prevalence. Harmful Algae 114, 102207. http://dx.doi.org/10.1016/j.hal.2022.102207.

Ma, Z.L., Wang, C.X., Qin, W.L., Wang, M., Chen, B.B., Jia, Y., Qin, Z.X., Dai, C.J., Yu, H.G., Li, G., Li, R.H., Thring, W.R., Zhao, M., 2021. Inhibitory effects of *Prorocentrum donghaiense* allelochemicals an sargassum fusiformis zygotes probed by Jip-Test based on fast chlorophyll fluorescence kinetics. Mar. Environ. Res. 170, http://dx.doi.org/10.1016/j.marenvres.2021.105453.

Mackey, M., Glass, L., 1977. Oscillation and chaos in physiological control systems. Science 197, 287–289. http://dx.doi.org/10.1126/science.267326.

Mclaughlin, K., Sohm, J.A., Cutter, G.A., Lomas, M.W., Paytan, A., 2013. Phosphorus cycling in the Sargasso Sea: Investigation using the oxygen isotopic composition of phosphate, enzyme-labeled fluorescence, and turnover times. Global Biogeochem. Cycles 27, 375–387. http://dx.doi.org/10.1002/GBC.20037.

Melendez-Alvarez, J., He, C., Zhang, R., Kuang, Y., Tian, X.J., 2021. Emergent oscillation induced by nutrient-modulating growth feedback. ACS Synth. Biol. 10, 1227–1236. http://dx.doi.org/10.1101/2021.02.09.430447.

Misra, A.N., Misra, M., Singh, R., 2012. Chlorophyll Fluorescence in Plant Biology. Biophysics.

Misra, A.K., Singh, R.K., Tiwari, P.K., Khajanchi, S., Kang, Y., 2020. Dynamics of algae blooming: effects of budget allocation and time delay. Nonlinear Dynam. 100, http://dx.doi.org/10.1007/s11071-020-05551-4.

Monod, J., 1949. The growth of bacterial cultures. Annu. Rev. Microbiol. 3, 371–394. http://dx.doi.org/10.1146/annurev.mi.03.100149.002103.

Nikolaou, A., Hartmann, P., Sciandra, A., Chachuat, B., Bernard, O., 2016. Dynamic coupling of photoacclimation and photoinhibition in a model of microalgae growth. J. Theoret. Biol. 390, 61–72. http://dx.doi.org/10.23919/ecc.2013.6669381.

Ou, L.J., Wang, D., Huang, B.Q., Hong, H.S., Qi, Y.Z., Lu, S.H., 2008. Comparative study of phosphorus strategies of three typical harmful algae in Chinese coastal waters. J. Plankton Res. 30, 1007–1017. http://dx.doi.org/10.1093/plankt/fbn058.

Parkhill, J.P., Maillet, G., Cullen, J.J., 2001. Fluorescence-based maximal quantum yield for PSII as a diagnostic of nutrient stress. J. Phycol. 37, 517–529. http://dx.doi.org/10.1046/j.1529-8817.2001.037004517.x.

Peace, A., Wang, H., 2019. Compensatory foraging in stoichiometric producer–grazer models. Bull. Math. Biol. 81, 4932–4950. http://dx.doi.org/10.1007/s11538-019-00665-2.

Qi, H.J., Wang, J.T., Wang, Z.Y., 2013. A comparative study of the sensitivity of F_v/F_m to phosphorus limitation on four marine algae. J. Ocean U. China 12, 77–84. http://dx.doi.org/10.1007/s11802-011-1975-5.

Qiu, X.C., Shimasaki, Y., Tsuyama, M., Yamada, T., Kuwahara, R., Kawaguchi, M., Honda, M., Gunjikake, H., Tasmin, R., Shimizu, M., et al., 2013. Growth-phase dependent variation in photosynthetic activity and cellular protein expression profile in the harmful raphidophyte *Chattonella antiqua*. Biosci. Biotech. Bioch. 77, 46–52. http://dx.doi.org/10.1271/bbb.120543.

Sañudo-Wilhelmy, S.A., Tovar-Sanchez, A., Fu, F.X., Capone, D.G., et al., 2004. The impact of surface-adsorbed phosphorus on phytoplankton Redfield stoichiometry. Nature 432, 897–901. http://dx.doi.org/10.1038/nature03125.

Schreiber, U., Gademann, R., Ralph, P.J., Larkum, A.W.D., 1997. Assessment of photosynthetic performance of *Prochloron* in *Lissoclinum* patella in hospite by chlorophyll fluorescence measurements. Plant Cell Physiol. 38, 945–951. http://dx.doi.org/10.1093/oxfordjournals.pcp.a029256.

Schreiber, U., Schliwa, U., Bilger, W., 1986. Continuous recording of photochemical and non-photochemical chlorophyll fluorescence quenching with a new type of modulation fluorometer. Photosynth. Res. 10, 51–62. http://dx.doi.org/10.1002/2016JC012368.

Shen, A.L., Chen, W.W., Xu, Y.J., Ho, K.C., 2022. Zooplankton population and community structure changes in response to a harmful algal bloom caused by *Prorocentrum donghaiense* in the East China Sea. J. Mar. Sci. Eng. 10, 291. http://dx.doi.org/10.3390/jmse10020291.

Shen, A.L., Ishizaka, J., Yang, M.M., Ouyang, L.L., Yin, Y., Ma, Z.L., 2019. Changes in community structure and photosynthetic activities of total phytoplankton species during the growth, maintenance, and dissipation phases of a *Prorocentrum donghaiense* bloom. Harmful Algae 82, 35–43. http://dx.doi.org/10.1016/j.hal.2018.12.007.

Shen, A.L., Li, D.J., 2016. Effects of different nutrients levels on the growth of *Prorocentrum donghaiense* and *Karenia mikimotoi*. Mar. Fish. 38, 416–422 (in Chinese with English abstract).

Shen, A.L., Ma, Z.L., Jiang, K.J., Li, D.J., 2016. Effects of temperature on growth, photophysiology, Rubisco gene expression in *Prorocentrum donghaiense* and *Karenia mikimotoi*. Ocean Sci. J. 51, 581–589. http://dx.doi.org/10.1007/s12601-016-0056-2.

Shi, P.L., Shen, H., Wang, W.J., Yang, Q., Xie, P., 2016. Habitat-specific differences in adaptation to light in freshwater diatoms. J. Appl. Phycol. 28, 227–239. http://dx.doi.org/10.1007/s10811-015-0531-7.

Shin, H.H., Li, Z., Mertens, K.N., Min, H.S., Matsuoka, K., 2019. *Prorocentrum shikokuense* Hada and *P. donghaiense* Lu are junior synonyms of *P. obtusidens* schiller, but not of *P. dentatum* Stein (Prorocentrales, Dinophyceae). Harmful Algae 89, 101686. http://dx.doi.org/10.1016/j.hal.2019.101686.

Song, D., Fan, M., Chen, M., Wang, H., 2019. Dynamics of a periodic stoichiometric model with application in predicting and controlling algal bloom in Bohai Sea off China. Math. Biosci. Eng. 16, 119–138. http://dx.doi.org/10.3934/mbe.2019006.

Sourav, Kumar, Sasmal, Yasuhiro, Takeuchi, 2020. Dynamics of a predator-prey system with fear and group defense. J. Math. Anal. Appl. 481, 123471. http://dx.doi.org/10.1016/j.jmaa.2019.123471.

Springer, J.J., Burkholder, J.M., Glibert, P.M., Reed, R.E., 2005. Use of a real-time remote monitoring network (RTRM) and shipborne sampling to characterize a dinoflagellate bloom in the Neuse Estuary, North Carolina, USA. Harmful Algae 4, 533–551. http://dx.doi.org/10.1016/j.hal.2004.08.017.

Straka, L., Rittmann, B.E., 2018. Light-dependent kinetic model for microalgae experiencing photoacclimation, photodamage, and photodamage repair. Algal Res. 31, 232–238. http://dx.doi.org/10.1016/j.algal.2018.02.022.

Sun, J., Liu, D.Y., Ning, X.R., Liu, C.G., 2003. Phytoplankton in the Prydz Bay and the adjacent Indian sector of the southern ocean during the austral summer 2001/2002. Oceanologia Et Limnologia Sinica 34, 519–532. http://dx.doi.org/10.1023/A:1022289509702.

Sun, K., Qiu, Z.F., He, Y.J., Fan, W., Wei, Z.X., 2017. Vertical development of a prorocentrum donghaiense bloom in the coastal waters of the East China Sea: coupled biophysical numerical modeling. Acta Oceanol. Sin. 36, 1–11. http://dx.doi.org/10.1007/s13131-016-0965-z.

Tao, B.Y., Mao, Z.H., Lei, H., Pan, D.L., Bai, Y., Zhu, Q.k., Zhang, Z.L., 2017. A semianalytical MERIS green-red band algorithm for identifying phytoplankton bloom types in the East China Sea. J. Geophys. Res.-Oceans 122, 1772–1788. http://dx.doi.org/10.1002/2016JC012368.

Tao, B.Y., Mao, Z.H., Lei, H., Pan, D.L., Shen, Y.Z., Bai, Y., Zhu, Q.K., Li, Z.E., 2015. A novel method for discriminating *Prorocentrum donghaiense* from diatom blooms in the East China Sea using MODIS measurements. Remote Sens. Environ. 158, 267–280. http://dx.doi.org/10.1016/j.rse.2014.11.004.

Wang, X.L., Deng, N.N., Zhu, C.J., Han, X.R., Li, K.Q., Xin, Y., Chen, L.L., 2004. Effect of nutrients (Phosphate and Nitrate) composition on the growth of HAB algae. J. Ocean Univer. China 3, 453–460. http://dx.doi.org/10.16441/j.cnki.hdxb.2004.03.016, (in Chinese with English abstract).

Wang, H., Smith, H., Kuang, Y., Elser, J., 2007. Dynamics of stoichiometric bacteria-algae interactions in the epilimnion. SIAM J. Appl. Math. 68, 503–522. http://dx.doi.org/10.1137/060665919.

Wang, Z.Y., Wang, J.T., Tan, L.J., 2014. Variation in photosynthetic activity of phytoplankton during the spring algal blooms in the adjacent area of Changjiang River estuary. Ecol. Indic. 45, 465–473. http://dx.doi.org/10.1016/j.ecolind.2014.05.010.

Wang, Y.H., Wu, H., Gao, L., Shen, F., Liang, X.S., 2019. Spatial distribution and physical controls of the spring algal blooming off the Changjiang River Estuary. Estuar. Coast. 42, 1066–1083. http://dx.doi.org/10.1007/s12237-019-00545-x.

Wang, H., Zhu, R., Zhang, J., Ni, L., Shen, H., Xie, P., 2018. A novel and convenient method for early warning of algal cell density by chlorophyll fluorescence parameters and its application in a highland lake. Front. Plant Sci. 9, 869. http://dx.doi.org/10.3389/fpls.2018.00869.

Wu, J., Sunda, W., Boyle, E.A., Karl, D.M., 2000. Phosphate depletion in the Western North Atlantic Ocean. Science 289, 759–762. http://dx.doi.org/10.1126/science.289.5480.759.

Xu, D.Q., Zhang, Y.Z., Zhang, R.X., 1992. Photoinhibition of photosynthesis in plants. Plant Physiol. Commun. 4, 237–243. http://dx.doi.org/10.13592/j.cnki.ppj.1992.04.001, (in Chinese with English abstract).

Yan, Y.W., Zhang, J.M., Wang, H., 2021. Dynamics of stoichiometric autotroph-mixotroph-bacteria interactions in the epilimnion. Bull. Math. Biol. 84, http://dx.doi.org/10.1007/s11538-021-00962-9.

Yuan, S.L., Wu, D.M., Lan, G.J., Wang, H., 2020. Noise-induced transitions in a nonsmooth Producer–Grazer model with stoichiometric constraints. Bull. Math. Biol. 82, 1–22. http://dx.doi.org/10.1007/s11538-020-00733-y.

Zhang, H., He, Y.B., Wu, P.F., Zhang, S.F., Xie, Z.X., Li, D.X., Lin, L., Chen, F., Wang, D.Z., 2019a. Comparative metaproteomics reveals functional differences in the blooming phytoplankton *Heterosigma akashiwo* and *Prorocentrum donghaiense*. Appl. Environ. Microbiol. http://dx.doi.org/10.1128/AEM.01425-19, AEM–01425.

Zhang, J.M., Kong, J.D., Shi, J., Wang, H., 2021. Phytoplankton competition for nutrients and light in a stratified lake: a mathematical model connecting epilimnion and hypolimnion. J. Nonlinear Sci. 31, http://dx.doi.org/10.1007/s00332-021-09693-6.

Zhang, Y.Q., Lin, X., Shi, X.G., Lin, L.X., Luo, H., Li, L., Lin, S.J., 2019b. Meta-transcriptomic signatures associated with phytoplankton regime shift from diatom dominance to a dinoflagellate bloom. Front. Microbiol. 10, 590. http://dx.doi.org/10.3389/fmicb.2019.00590.

Zhang, S.F., Yuan, C.J., Chen, Y., Lin, L., Wang, D.Z., 2019c. Transcriptomic response to changing ambient phosphorus in the marine dinoflagellate *Prorocentrum donghaiense*. Sci. Total Environ. 692, 1037–1047. http://dx.doi.org/10.1016/j.scitotenv.2019.07.291.

Zhao, S.N., Yuan, S.L., Wang, H., 2020. Threshold behavior in a stochastic algal growth model with stoichiometric constraints and seasonal variation. J. Differential Equations 268, 5113–5139. http://dx.doi.org/10.1016/j.jde.2019.11.004.